JBAAR
Journal of Basic and Applied Research in Biomedicine
ISSN 2413-7014

Original Article

Dual Action of Avarol Quinone Terpenoid: Disrupting Cell Wall and Membrane Integrity in *Staphylococcus aureus*

Syed Z. Idid[1], Shahbudin Saad[2], Deny Susanti[3]

[1]Faculty of Allied Health Sciences, International Islamic University Malaysia, Kuantan, Pahang, Malaysia
[2]Department of Marine Science, Faculty of Science, International Islamic University Malaysia, Kuantan, Pahang, Malaysia
[3]Department of Chemistry, Faculty of Science, International Islamic University Malaysia, Kuantan, Pahang, Malaysia

*Corresponding Author: syedzahir@iiu.edu.my

Received: 22-07-2025
Revised: 19-08-2025
Published: 26-08-2025

Keywords:
Avarol quinone terpenoid;
Staphylococcus aureus;
Antibacterial mechanism;
Cell membrane disruption;
Cell wall targeting;
Ion leakage;
ATP depletion;
Autolysis;
Membrane depolarization

Abstract: The rising threat of multidrug-resistant bacteria necessitates the discovery of novel antibacterial agents with distinct mechanisms of action. In this study, we investigated the antibacterial activity and mechanism of action of Avarol Quinone Terpenoid (AQT), a polyfunctional compound isolated from the marine sponge *Neopetrosia exigua*, against *Staphylococcus aureus* ATCC 25923. Minimum inhibitory concentration (MIC) testing revealed that AQT exhibits bacteriostatic activity at 2.6 µg/mL and bactericidal activity at 5.2 µg/mL. To further explore its antibacterial mechanism, a series of in vitro assays were performed to assess its impact on bacterial viability, morphology, membrane integrity, and cellular metabolism. Time-kill analysis demonstrated a concentration-dependent reduction in *S. aureus* viability. Scanning electron microscopy (SEM) revealed severe morphological alterations in AQT-treated cells, including membrane deformation and collapse. Membrane permeability was significantly increased, as indicated by elevated uptake of crystal violet and propidium iodide dyes. These effects were accompanied by marked leakage of nucleic acids, proteins, potassium, calcium, and ATP, supporting membrane disruption. SDS-PAGE analysis showed reduced total protein content, although lipase activity remained unaffected, suggesting AQT does not inhibit protein synthesis. API Staph tests indicated that AQT inhibited sugar utilization (lactose, maltose, and N-acetylglucosamine) and suppressed arginine dihydrolase activity, potentially impairing ATP generation. Autolysis assays showed increased activity of cell wall-degrading enzymes, consistent with cell wall-targeting antibiotics. Furthermore, membrane depolarization assays using $DiSC_3(5)$ confirmed the dissipation of membrane potential. Collectively, these findings suggest that AQT exerts its antibacterial effects through a multifaceted mechanism targeting both the cell wall and the cytoplasmic membrane, leading to loss of membrane integrity, energy depletion, and bacterial cell death. AQT thus holds promise as a potential anti-*S. aureus* therapeutic agent.

Cite this article as: Idid, S.Z., Saad, S., Susanti, D. (2025) Dual Action of Avarol Quinone Terpenoid: Disrupting Cell Wall and Membrane Integrity in *Staphylococcus aureus*. Journal of Basic and Applied Research in Biomedicine, 11(1): 20-29.

This work is licensed under a Creative Commons Attribution 4.0 License. You are free to copy, distribute and perform the work. You must attribute the work in the manner specified by the author or licensor.

INTRODUCTION

The mechanisms of action of newly discovered antibiotics are typically investigated after determining whether they exhibit bacteriostatic or bactericidal activity. Agents demonstrating potent activity are subsequently evaluated for their selectivity and toxicity (Chen et al., 2024; Dalhoff, 2021). Given the various modes of action of antibiotics, a new antibiotic agent may target the cell wall, cell membrane, or intracellular processes involved in macromolecular synthesis, such as DNA, RNA, protein, or lipid synthesis (Allison & Lambert, 2024).

Several methodological strategies have been developed to investigate the modes of action of antibiotics, and significant progress has been made in understanding their mechanisms. Advanced approaches such as DNA chip technologies and proteome analyses focus on all cellular components and their interactions (systems biology), while other strategies target individual components, including genes, proteins, and biochemical pathways (Ideker et al., 2001; Priyamvada et al., 2022). Numerous techniques are available for studying the effects of antibiotics on individual cellular components. These include microscopic examination, analysis of cell lysis, leakage of intracellular constituents, enzyme inhibition, ion and electron transport systems, changes in membrane potential, oxidative phosphorylation, and macromolecular biosynthetic processes (Ann-Britt et al., 2024; de León et al., 2010; Devi et al., 2010; Ren et al., 2024; Zhou et al., 2008). Singh and Barrett (2006) recommended that studies on the mode of action should not focus solely on previously identified mechanisms or predefined targets. Instead, comprehensive screening against the entire bacterial structure is preferable for accurately verifying antibacterial activity (Singh & Barrett, 2006).

Naturally occurring antibiotics often possess complex structural scaffolds and multiple functional groups, enabling them to interact with various molecular targets (Brötz-Oesterhelt & Brunner, 2008; Sharma et al., 2025). Marine natural products, in particular, exhibit unique and diverse chemical structures enriched with significant functional groups. Compounds containing groups such as hydroxyl, sulfate, carboxyl, and ester moieties have been associated with potent antibacterial activity. Additionally, hydrocarbon side chains are believed to enhance antimicrobial effects. The number and position of these functional groups are considered critical factors in modulating and enhancing antibacterial activity (Togashi et al., 2007; Ul Haq et al., 2024).

Quinone terpenoids typically feature a trans-decalin system within a rearranged drimane skeleton. However, their structures can vary depending on the presence or absence of double bonds, the position of these bonds, and the substitution pattern on the quinone ring (Sladić & Gasić, 2006). An unusual polyfunctional quinone, avarol quinone terpenoid (AQT), was isolated from the marine sponge *Neopetrosia exigua* and demonstrated potent antibacterial activity (Idid et al., 2024). AQT comprises a bicyclic sesquiterpene skeleton attached to a quinone moiety (Figure 1), although the presence of a bicyclic system is not a prerequisite for significant antimicrobial activity. While structurally related to avarol, AQT features additional functional modifications within both the hydrophobic terpene unit and the quinone ring. The sesquiterpene skeleton includes two key

functional groups: a hydroxyl group at C-3 and an aliphatic side chain with a terminal carboxylic acid group at C-4. The quinone moiety contains two sulfate ester groups. Given the presence of hydroxyl, sulfate, carboxylic acid, and ester functionalities, it is not surprising that AQT exhibits strong antimicrobial activity. The antibacterial mechanism of action for lipophilic compounds such as quinone terpenoids—particularly against Gram-positive bacteria like *Staphylococcus aureus*—is primarily attributed to disruption of the bacterial cell membrane (Sladić & Gasić, 2006; Zhao et al., 2023).

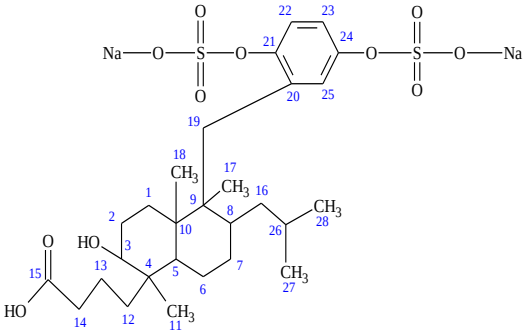

Figure 1: chemical structure of avarol quinone terpenoid (AQT).

It is plausible that AQT exhibits bactericidal activity through a sequence of events initiated by its interaction with the bacterial cell surface—beginning with surface binding, followed by penetration of the cell wall and membrane, and ultimately interaction with cytoplasmic constituents (Devi et al., 2010; Zhou et al., 2008). The objectives of this study are to assess the effectiveness of AQV in inhibiting the growth and survival of *Staphylococcus aureus*, and to evaluate the mode of its bactericidal action against *S. aureus*.

MATERIALS AND METHODS

Avarol quinone terpenoid (AQT) and *S. aureus*

Avarol quinone terpenoid (AQT) was isolated from the marine sponge *Neopetrosia exigua*, as previously reported (Idid et al., 2024). In all experiments, AQT was prepared in dimethyl sulfoxide (DMSO). *Staphylococcus aureus* ATCC 25923 was obtained from the American Type Culture Collection.

Bacterial Killing Assay

The bacterial killing assay was performed based on the method described by (Carson et al., 2002), with slight modifications. The antibacterial activity of AQT against *Staphylococcus aureus* was assessed by monitoring colony-forming units (CFU) per milliliter over a 16-hour period. *S. aureus* cultures were grown to the exponential phase (10^7 CFU/mL) and treated with AQT at various concentrations: the minimum inhibitory concentration (MIC; 2.6 µg/mL), ½ MIC (1.3 µg/mL), 2× MIC (5.2 µg/mL), and 4× MIC (10.4 µg/mL). Cultures were incubated at 37 °C, and 100 µL samples were withdrawn at designated time intervals (0, 2, 4, 6, 8, 10, 12, 14, and 16 h), serially diluted, and plated onto Mueller-Hinton agar (MHA). After 24 hours of incubation at 37 °C, the number of surviving colonies was recorded. An untreated *S. aureus* culture served as the negative control. All experiments were conducted in triplicate.

Scanning Electron Microscopy (SEM)

Scanning electron microscopy (SEM) analysis was carried out following the methods of (Benli et al., 2008) and (Devi et al., 2010), with slight modifications. *S. aureus* cultures grown to the exponential phase (10^7 CFU/mL) were treated with AQT at concentrations equivalent to 2× MIC (5.2 µg/mL) and 4× MIC (10.4 µg/mL) for 3 hours at 37 °C. Following treatment, cells were harvested by centrifugation at 9300×g for 25 minutes, washed twice with phosphate-buffered saline (PBS, pH 7.4), and fixed in 2.5% glutaraldehyde prepared in PBS. The fixed cells were then dehydrated through a graded ethanol series, dried, and coated with carbon using an ion sputter coater. Samples were examined using a scanning electron microscope at an accelerating voltage of 20 kV. Untreated cells were prepared in the same manner and used as a control.

Cell Lysis Assay

Autolysis assays for treated and untreated *S. aureus* were performed as previously described, with slight modifications (Hanaki et al., 1998; Mani et al., 1993). *S. aureus* cultures grown to the exponential phase (10^7 CFU/mL) were treated with AQT at a concentration of 10.4 µg/mL for 3 hours at 37 °C. After treatment, 1 mL cell samples from both treated and untreated cultures were collected and pelleted by centrifugation. The cells were washed twice with 1 mL of ice-cold distilled water and re-suspended in 1 mL of 0.05 M Tris-HCl buffer (pH 7.2) containing 0.05% (v/v) Triton X-100. The suspensions were incubated at 37 °C, and the absorbance at 580 nm (OD_{580}) was measured at designated time intervals over a 4-hour period. Cell lysis was determined by the decrease in OD_{580} and expressed as a percentage of the initial value (0 h) using the formula:

(OD_{580} at each time point / OD_{580} at 0 h) × 100%

Crystal Violet Assay

The crystal violet uptake assay was performed following the method of (Devi et al., 2010), with minor modifications. *S. aureus* cultures grown to the exponential phase (10^7 CFU/mL) were harvested by centrifugation at 4500×g for 5 minutes at 4°C. The cell pellets were washed twice and re-suspended in phosphate-buffered saline (PBS, pH 7.4). AQT was added to the suspensions at concentrations of 5.2 and 10.4 µg/mL. Control samples were prepared without AQT, while cells treated with 0.25 M EDTA served as a positive control. Following 30 minutes of incubation at 37 °C, the cells were harvested by centrifugation at 9300×g for 5 minutes and re-suspended in PBS containing crystal violet (5 µg/mL). The suspensions were incubated for an additional 10 minutes at 37 °C, followed by centrifugation at 13,400×g for 15 minutes. The absorbance of the supernatants was then measured at 590 nm using a spectrophotometer. The optical density (OD) of the crystal violet stock solution (5 µg/mL) was considered as 100%. The percentage of crystal violet uptake by treated and untreated cells was calculated using the formula:

% Crystal violet uptake = (OD_{590} of the sample / OD_{590} of the crystal violet stock solution) × 100%

Propidium Iodide (PI) Assay

Membrane permeability was assessed following the methods of (Gauri et al., 2011; Joshi et al., 2010), with slight modifications. *S. aureus* cultures grown to the exponential phase (10^7 CFU/mL) were washed three times and re-suspended in phosphate-buffered saline (PBS, pH 7.4). The bacterial suspensions were then treated with AQT at concentrations of 5.2 and 10.4 µg/mL for 30 minutes, followed by incubation with propidium iodide (PI) at a final concentration of 10 µg/mL for another 30 minutes. Fluorescence intensity was measured using a fluorescence plate reader at an excitation wavelength of 535 nm and an emission wavelength of 617 nm.

Leakage of 260 nm Absorbing Material

The release of UV-absorbing materials was measured using a spectrophotometer according to the method of (Zhou et al., 2008), with minor modifications. *Staphylococcus aureus* cultures grown to the exponential phase (10^7 CFU/mL) were washed three times and re-suspended in phosphate-buffered saline (PBS, pH 7.4). Bacterial suspensions (1 mL) were incubated with AQT at two different concentrations (5.2 and 10.4 µg/mL). Chloramphenicol and streptomycin were included as reference antibiotics for comparison, and untreated *S. aureus* served as a control. After 60 minutes of incubation at 37 °C, the suspensions were centrifuged at 13,400×g for 15 minutes. The optical density of the supernatants was measured at 260 nm (OD_{260}) to determine the release of extracellular UV-absorbing materials. All measurements were performed in triplicate.

Loss of 280 nm Absorbing Material

S. aureus cultures grown to the exponential phase (10^7 CFU/mL) were washed three times and re-suspended in phosphate-buffered saline (PBS, pH 7.4). One milliliter of the bacterial suspension was incubated with AQT at two different concentrations (5.2 and 10.4 µg/mL). Chloramphenicol and

streptomycin were included as reference antibiotics for comparison, while untreated *S. aureus* served as a control. Following 60 minutes of incubation at 37 °C, the suspensions were centrifuged at 13,400×g for 15 minutes. The absorbance of the supernatant was measured at 280 nm to assess the release of extracellular UV-absorbing materials. All experiments were conducted in triplicate.

Leakage of Potassium and Calcium Ions

The extracellular and intracellular concentrations of potassium (K^+) and calcium (Ca^{2+}) ions were determined using inductively coupled plasma mass spectrometry (ICP-MS). Cell preparation was performed according to (Zhou et al., 2008), with minor modifications. *S. aureus* cultures grown to the exponential phase (10^7 CFU/mL) were treated with AQT at a concentration of 5.2 µg/mL and incubated at 37 °C. At designated time points (0, 1.5, and 3 hours), 1 mL samples from both treated and untreated cultures were collected and immediately chilled on ice. Samples were centrifuged at 6000×g for 10 minutes at 0 °C, and the supernatants were collected for determination of extracellular K^+ and Ca^{2+} concentrations. The resulting cell pellets were re-suspended in 1 mL of 5% (w/v) trichloroacetic acid and stored at −20 °C for 24 hours. Samples were then thawed and heated at 95 °C for 10 minutes. Subsequently, 4 mL of deionised water was added to each sample, followed by centrifugation at 10,000×g for 15 minutes. The resulting supernatants were used for intracellular K^+ and Ca^{2+} measurements. All ion concentrations were determined using ICP-MS.

SDS–PAGE of Whole-cell Proteins

S. aureus cultures grown to the exponential phase (10^7 CFU/mL) were treated with AQT at concentrations of 5.2 and 10.4 µg/mL for 1 hour at 37 °C. Following treatment, 1 mL samples from each treated and untreated culture were collected and centrifuged. The resulting cell pellets were used to extract total cellular proteins using BugBuster™ Protein Extraction Reagent (Sigma, USA), following the manufacturer's instructions. Protein concentrations in the extracts were determined using the Bradford assay. Equal amounts of protein from each sample were subjected to SDS–PAGE using a vertical electrophoresis system. The electrophoresis was carried out with a 4% stacking gel and a 10% separating gel. Protein bands were visualized by staining with Coomassie Brilliant Blue R-250 according to the manufacturer's protocol.

Measurement of ATP Levels

Intracellular and extracellular ATP levels of *S. aureus* treated with AQT and untreated controls were qualitatively measured according to the method described by (Fleury et al., 2009). *S. aureus* cultures grown to the exponential phase (10^7 CFU/mL) were treated with AQT at concentrations of 5.2 and 10.4 µg/mL for 3 hours at 37 °C. At appropriate time points, 1 mL samples were collected from each culture for intracellular ATP analysis. These samples were centrifuged, and the pellets were re-suspended in 1 mL of fresh Mueller-Hinton Broth (MHB). The supernatants were then filter-sterilized and transferred into new tubes for extracellular ATP analysis.

For ATP measurement, both intracellular and extracellular samples were assessed using the BacTiter-Glo™ Microbial Cell Viability Assay (Promega), following the manufacturer's instructions. In each well of a white 96-well plate (Microlite™ TCT, Promega), 100 µL of either bacterial extract or filter-sterilized supernatant was mixed with 100 µL of BacTiter-Glo™ reagent. Luminescence was measured using a fluorometer. All samples were tested in triplicate.

API Test System

To analyze the physiological changes in *Staphylococcus aureus* treated with AQT at concentrations of 5.2 and 10.4 µg/mL, the API Staph test system was employed following the manufacturer's instructions.

Lipase Production

Lipase activity was assessed to evaluate the effect of AQT on *S. aureus* lipid synthesis. The assay was performed using Agar Salty Tween (AST) plates as described by (Nostro et al., 2001), with the following composition: peptone (10.0 g/L), NaCl (75.0 g/L), $CaCl_2 \cdot 2H_2O$ (0.10 g/L), and Tween-80 (10.0 g/L), adjusted to pH 7.2. Aliquots of 100 µL of *S. aureus* suspension (10^7 CFU/mL) were plated onto AST plates, as well as AST plates supplemented with AQT at concentrations of 5.2 and 10.4 µg/mL. Following incubation for 24 hours at 37 °C, colonies exhibiting positive lipase activity were counted on each plate. The number of lipase-positive colonies on AQT-treated plates was compared to those on untreated AST plates, and results were expressed as a percentage of lipase activity (Barros et al., 2009).

Membrane Depolarization

Depolarization of the cytoplasmic membrane was assessed using the membrane potential-sensitive cyanine dye $DiSC_3(5)$, as described by (Friedrich et al., 2000), with slight modifications. *S. aureus* cultures grown to the exponential phase (10^7 CFU/mL) were washed twice and re-suspended in 5 mM HEPES buffer (pH 7.2). To equilibrate intra- and extracellular potassium concentrations, 100 mM KCl was added to the suspension. $DiSC_3(5)$ was then added at a final concentration of 0.4 µM and incubated for 2–3 minutes to allow dye uptake and quenching, ensuring stabilization of fluorescence (indicating intact membrane potential with ~90% fluorescence reduction). After stabilization, AQT was added at concentrations of 5.2 and 10.4 µg/mL, and fluorescence intensity was monitored at 0, 2, and 4 hours using a fluorescence plate reader with excitation at 622 nm and emission at 670 nm. The membrane potential of AQT-treated *S. aureus* was compared to untreated controls and cells treated with tetracycline. All experiments were performed in triplicate.

Statistical Analysis

All experiments were conducted in triplicate, and the data are presented as mean ± standard deviation. Statistical significance between two groups was assessed using a two-tailed *t*-test (Microsoft Excel 2010). A *p*-value of less than 0.05 was considered statistically significant.

RESULTS

A previous investigation by our research group showed that the MIC of AQT against *S. aureus* was 2.6 µg/mL (Idid et al., 2024).

Killing Curves

Growth reduction of *S. aureus* was observed at all tested concentrations of AQT. Compared to the untreated control, growth inhibition increased in a concentration-dependent manner. As shown in Figure 2, approximately 3.0 and 1.8 $\log_{10}$ CFU/mL of *S. aureus* remained viable at the end of the incubation period when treated with AQT at 1.3 and 2.6 µg/mL, respectively. In contrast, treatment with 5.2 and 10.4 µg/mL of AQT resulted in the survival of *S. aureus* for only 6 and 8 hours, respectively. After 2 hours of exposure, growth reductions of approximately 6.2, 5.8, 4.5, and 1.8 $\log_{10}$ CFU/mL were recorded for AQT concentrations of 1.3, 2.6, 10.4, and 15.6 µg/mL, respectively.

Scanning Electron Microscope (SEM)

Scanning electron microscopy (SEM) images of untreated and AQT-treated *S. aureus* cells are presented in Figure 3. *S. aureus* was treated with AQT at concentrations of 5.2 and 10.4 µg/mL for 3 hours. Notable differences in cellular morphology were observed between untreated and treated cells. Untreated cells (Figure 3A-C) exhibited a typical rounded shape, clustered arrangement, and smooth, regular surfaces. Treatment with AQT at both concentrations induced significant morphological alterations. Treated cells displayed irregular shapes, membrane deformation, and signs of cellular collapse. At 5.2 µg/mL (Figure 3D-F), cells showed features such as invaginations (concave depressions), surface projections, and bud scars. In contrast, treatment with 10.4 µg/mL AQT (Figure 3G-I) resulted in more severe damage, with cells appearing highly deformed or completely lysed.

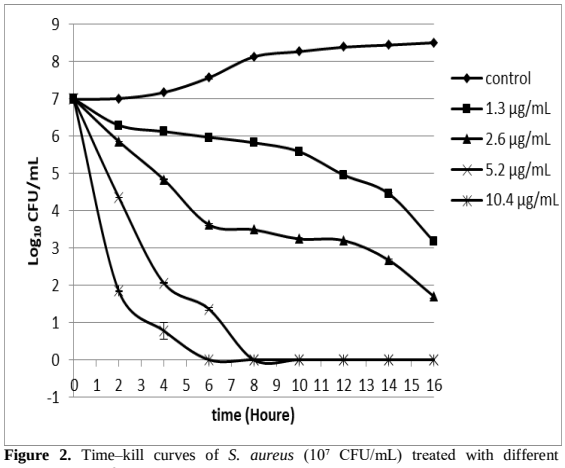

Figure 2. Time–kill curves of *S. aureus* (10^7 CFU/mL) treated with different concentrations of AQT compared to the untreated control. AQT was tested at ½ MIC (1.3 µg/mL), MIC (2.6 µg/mL), 2× MIC (5.2 µg/mL), and 4× MIC (10.4 µg/mL). Bacterial viability was monitored over time and expressed as $\log_{10}$ CFU/mL.

Cell Lysis

The rate of Triton X-100-induced autolysis was evaluated in untreated *S. aureus* cultures and those treated with 10.4 µg/mL AQT, 2 µg/mL chloramphenicol, or 2 µg/mL ampicillin. Overall, all treated cultures exhibited an increase in autolysis compared to the control, with the exception of the chloramphenicol-treated group. The autolysis rate generally increased with longer incubation times (Figure 4).

The untreated control culture showed a gradual reduction in cell density, with autolysis rates ranging from 84.9% to 46.6% over the incubation period. In comparison, *S. aureus* treated with 10.4 µg/mL AQT exhibited a more pronounced increase in autolysis, with rates declining from 53.6% to 24.1%. Similarly, ampicillin, a cell wall-targeting antibiotic, also enhanced autolysis (50.1% to 11.8%). In contrast, chloramphenicol, a protein synthesis inhibitor, induced minimal changes in autolysis, with rates remaining relatively stable (99.0% to 93.6%).

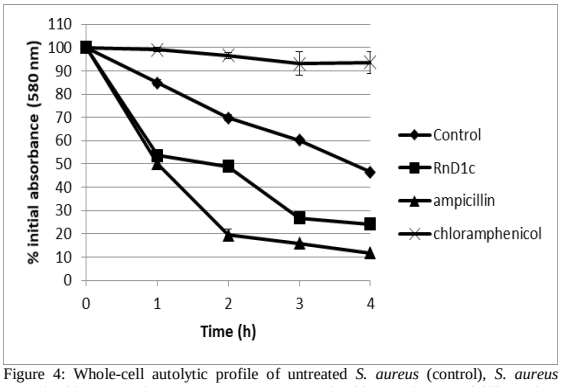

Figure 4: Whole-cell autolytic profile of untreated *S. aureus* (control), *S. aureus* treated with 10.4 µg/mL AQT, *S. aureus* treated with 2 µg/mL ampicillin and *S. aureus* treated with 2 µg/mL chloramphenicol.

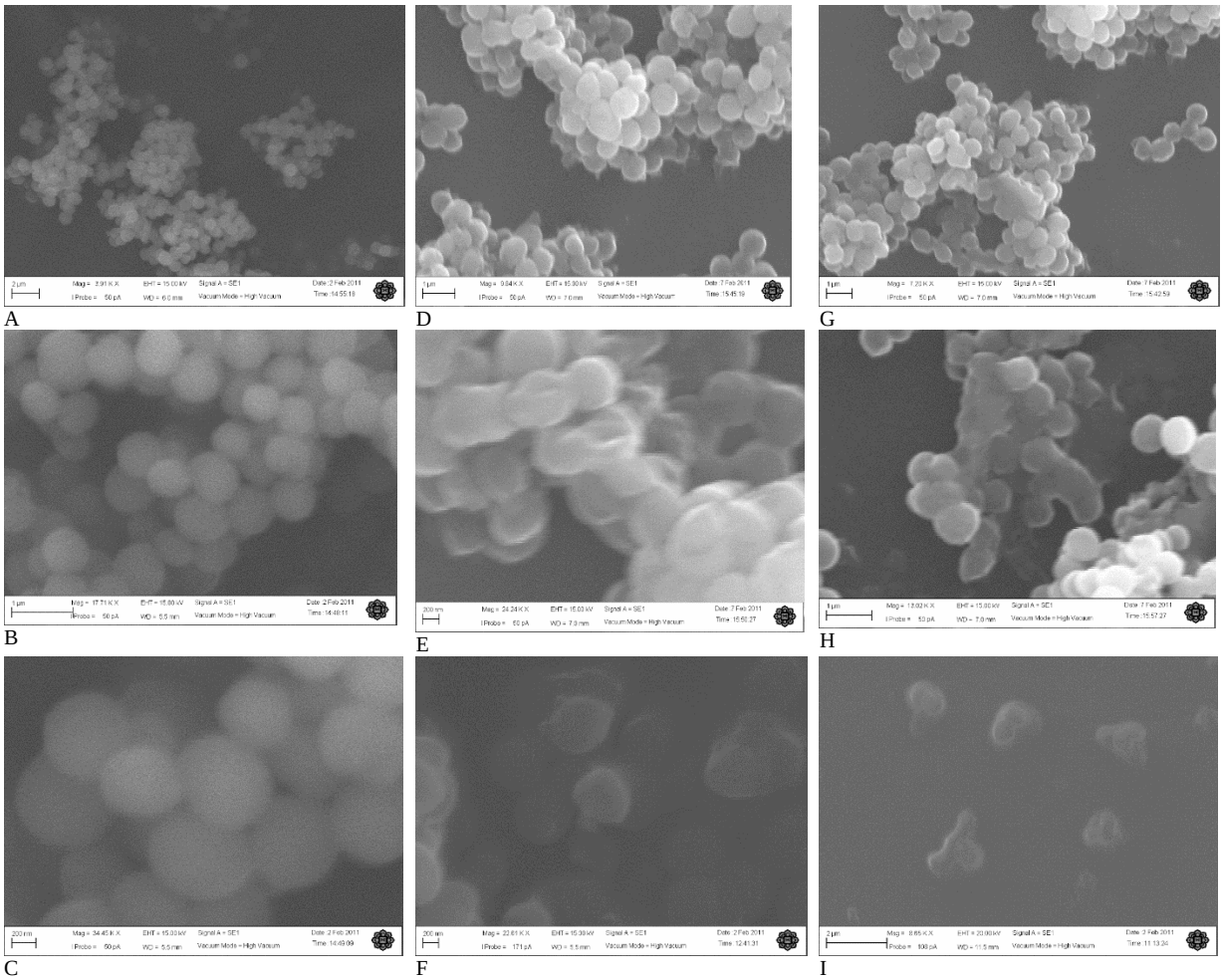

Figure 3: SEM micrographs of untreated *S. aureus* cells (A-C), *S. aureus* cells treated with 5.2 µg/mL AQT (D-F), and *S. aureus* cells treated with 10.4 µg/mL AQT (G-I).

Crystal Violet Assay

The crystal violet (CV) cell membrane assay was used to evaluate the membrane permeability of *S. aureus*. CV is a positively charged, non-toxic dye that can penetrate compromised cell membranes and bind to negatively charged cellular components such as DNA and phospholipids. To assess whether AQT affects membrane permeability, CV uptake by *S. aureus* treated with two concentrations of AQT was compared with uptake by untreated cells. Additional comparisons were made with cells treated with 0.25 M EDTA (a known membrane-disrupting chelating agent), as well as the antibiotics streptomycin and chloramphenicol.

As shown in Figure 5, CV uptake increased with increasing concentrations of AQT. Specifically, *S. aureus* treated with 5.2 µg/mL and 10.4 µg/mL AQT showed CV uptake of 10.76% and 21.35%, respectively. Cells treated with 0.25 M EDTA showed similarly high uptake (19.56%). In contrast, streptomycin- and chloramphenicol-treated cells exhibited significantly lower uptake values of 5.19% and 5.26%, respectively. These findings suggest that AQT compromises the integrity of the *S. aureus* cell membrane in a concentration-dependent manner, similar to the effect observed with EDTA, whereas streptomycin and chloramphenicol do not significantly affect membrane permeability.

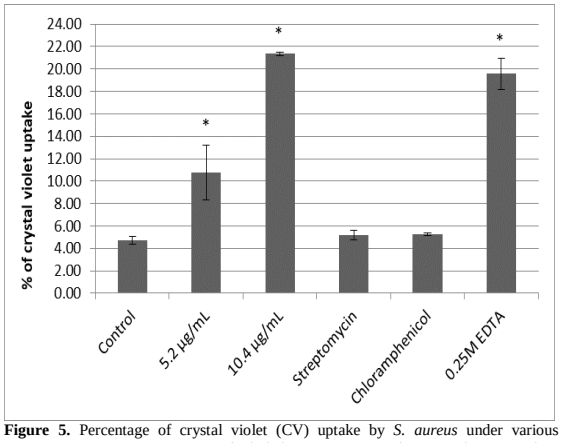

Figure 5. Percentage of crystal violet (CV) uptake by *S. aureus* under various treatment conditions. Treatments included AQT at 5.2 and 10.4 µg/mL, 2 µg/mL chloramphenicol, 2 µg/mL streptomycin, and 0.25 M EDTA. Untreated *S. aureus* served as the control. Increased CV uptake indicates enhanced membrane permeability.

PI Cytometry Assay

Membrane permeability of *S. aureus* was further evaluated using the fluorescent dye propidium iodide (PI). PI is a membrane-impermeable dye that selectively stains non-viable cells by intercalating into nucleic acids. In this assay, both treated and untreated *S. aureus* cells were stained with a fixed concentration of PI, and the percentage of PI uptake was used to assess membrane integrity.

The pattern of membrane permeability to PI was consistent with that observed in the crystal violet (CV) assay. A significant increase in PI uptake was observed in *S. aureus* treated with AQT, indicating compromised membrane integrity (Figure 6). In contrast, cells treated with chloramphenicol or streptomycin showed no significant increase in PI uptake compared to the untreated control, while treatment with 0.25 M EDTA resulted in a marked increase, serving as a positive control for membrane disruption.

Leakage of Cellular Metabolites

Leakage of intracellular components was assessed by measuring the absorbance of cell supernatants at 260 nm and 280 nm. *S. aureus* cultures were treated with AQT at concentrations of 5.2 and 10.4 µg/mL, and the results were compared with untreated cells as well as those treated with chloramphenicol and streptomycin. An increase in absorbance at 260 nm indicates the release of nucleic acids, while an increase at 280 nm reflects protein leakage.

As shown in Figure 7, there was significant leakage of extracellular 260 nm-absorbing materials from *S. aureus* treated with 10.4 µg/mL (A_{260} equal to 1.909), while it was not significant when it was treated with 5.2 µg/mL AQT (A_{260} equal to 1.534). Furthermore, there was also significant leakage of extracellular 260 nm-absorbing materials when *S. aureus* was treated with chloramphenicol (A_{260} equal to 3.481), while there was no significant difference in the leakage of 260 nm-absorbing materials when *S. aureus* was treated with streptomycin (A_{260} equal to 1.359) compared to untreated *S. aureus* (A_{260} equal to 1.288).

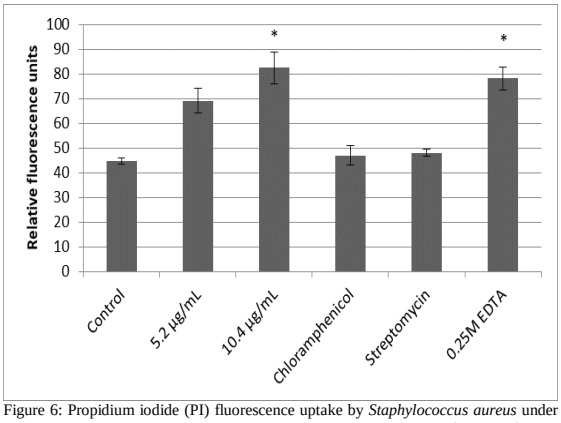

Figure 6: Propidium iodide (PI) fluorescence uptake by *Staphylococcus aureus* under various treatment conditions. Treatments included RnD1c at 5.2 and 10.5 µg/mL, 2 µg/mL chloramphenicol, 2 µg/mL streptomycin, and 0.25 M EDTA. Untreated *S. aureus* served as the control. Increased PI uptake indicates compromised membrane integrity and enhanced membrane permeability.

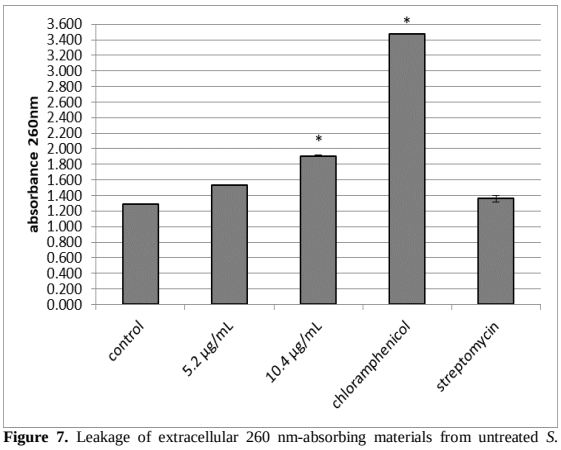

Figure 7. Leakage of extracellular 260 nm-absorbing materials from untreated *S. aureus*, *S. aureus* treated with 5.2 and 10.4 µg/mL AQT, *S. aureus* treated with 2 µg/mL chloramphenicol, and *S. aureus* treated with 2 µg/mL streptomycin. Increased absorbance at 260 nm indicates nucleic acid leakage and membrane damage.

As shown in Figure 8, significant leakage of extracellular 280 nm-absorbing materials occurred when *S. aureus* was treated with AQT at concentrations equal to 5.2 µg/mL (A_{280} equal to 0.519) and 10.4 µg/mL (A_{280} equal to 0.573). Chloramphenicol also caused significant leakage of extracellular 280 nm-absorbing materials (A_{280} equal to 0.765). However, there was no significant difference in the leakage of extracellular 280 nm-absorbing materials when *S. aureus* was treated with streptomycin (A_{280} equal to 0.423).

Leakage of Potassium Ions

To determine whether AQT has an impact on the extracellular K^+ concentration of *S. aureus*, the increase in extracellular K^+ was measured as an indicator of K^+ leakage. Generally, significant leakage of K^+ was observed when *S. aureus* was treated with 5.2 µg/mL AQT (Figure 9). The leakage of K^+ increased over the treatment period (0 to 3 h). Particularly, immediate K^+ leakage was observed (extracellular K^+ concentration was 2500 ppb), then the leakage dramatically increased after 1.5 h (3902 ppb), while it reached a maximum of 4250 ppb after a 3-hour incubation period.

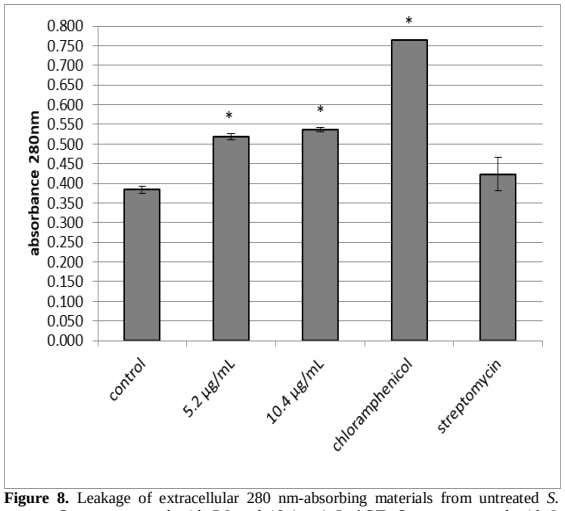

Figure 8. Leakage of extracellular 280 nm-absorbing materials from untreated *S. aureus*, *S. aureus* treated with 5.2 and 10.4 µg/mL AQT, *S. aureus* treated with 2 µg/mL chloramphenicol, and *S. aureus* treated with 2 µg/mL streptomycin. Increased absorbance at 280 nm indicates protein leakage due to membrane disruption.

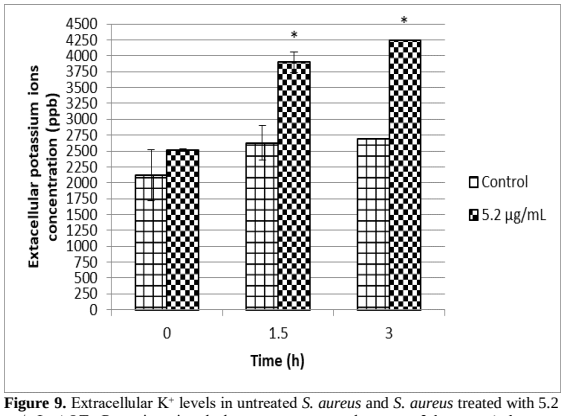

Figure 9. Extracellular K^+ levels in untreated *S. aureus* and *S. aureus* treated with 5.2 µg/mL AQT. Potassium ion leakage was measured over a 3-hour period as an indicator of membrane disruption.

Leakage of Calcium Ions

The percentage of Ca^{2+} leakage was measured in a similar way to that of K^+ leakage. *S. aureus* treated with 5.2 µg/mL AQT showed significant leakage of Ca^{2+} even at 0 h (Figure 10). The leakage of Ca^{2+} increased with the incubation period. About 30% of Ca^{2+} was lost immediately when *S. aureus* was treated with AQT; the percentage of leakage increased to 42% after 1.5 h, while it reached a maximum of 54% at the end of the experimental period.

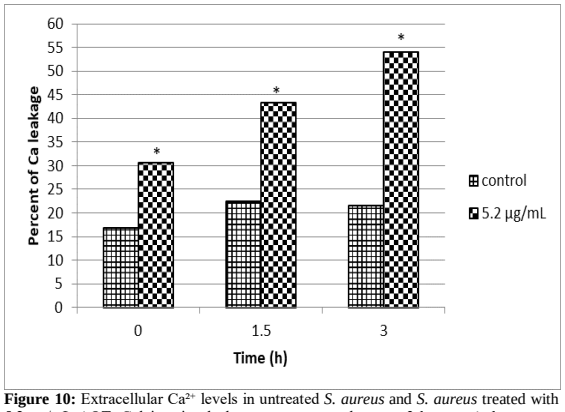

Figure 10: Extracellular Ca^{2+} levels in untreated *S. aureus* and *S. aureus* treated with 5.2 µg/mL AQT. Calcium ion leakage was measured over a 3-hour period to assess membrane disruption.

Whole Cell Protein Contents and SDS-PAGE

The whole cell proteins of treated and untreated *S. aureus* were extracted and subjected to SDS-PAGE at similar concentrations. The treated *S. aureus* yielded lower protein concentration compared to untreated *S. aureus*. Untreated *S. aureus* protein content (2.07 mg/mL) was about 2-fold higher than the treated *S. aureus* protein content (0.99 mg/mL). SDS-PAGE profiles showed significant differences in electrophoretic band patterns between untreated *S. aureus* and *S. aureus* treated with AQT. As shown in Figure 11, protein electrophoresis bands of untreated *S. aureus* appeared clear and intense, whereas the protein bands of *S. aureus* treated with 5.2 µg/mL AQT were markedly reduced, and some bands had disappeared. When *S. aureus* was treated with 10.4 µg/mL AQT, these effects became even more pronounced.

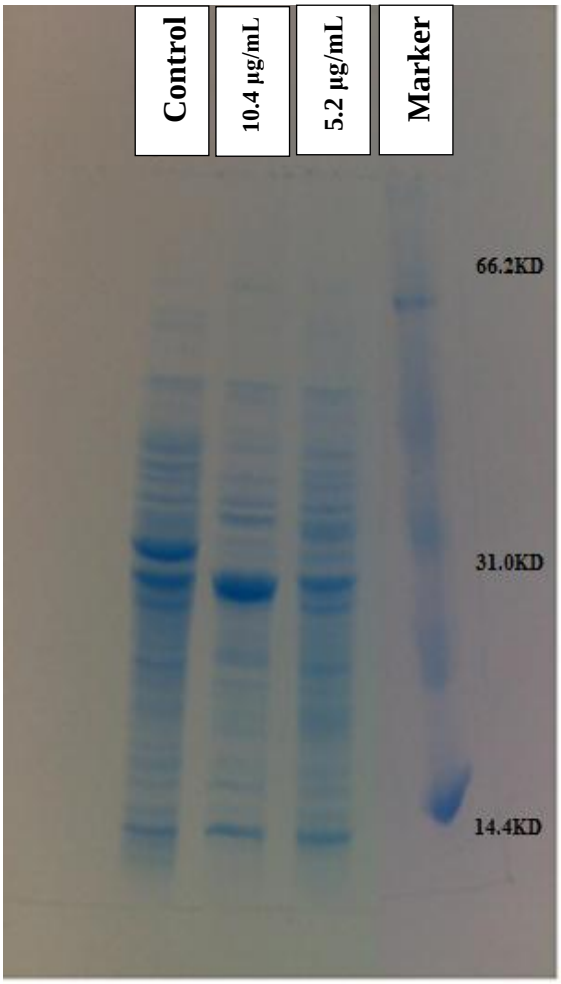

Figure 11: SDS-PAGE profile of total cellular proteins from untreated *S. aureus* and *S. aureus* treated with AQT at two different concentrations (5.2 and 10.4 µg/mL). Protein band intensity and pattern differences reflect AQT-induced effects on protein expression and/or synthesis.

Enzymatic Activities Using API Staph 20 Kit

The physiological status of *Staphylococcus aureus* treated with AQT at two different concentrations (5.2 and 10.4 µg/mL) was compared with untreated *S. aureus* using API Staph, which consists of 20 biochemical tests (Table 1). Among the enzymatic activities assessed with the API Staph system, only four tests were inhibited compared to untreated *S. aureus*. Particularly, sugar utilization (acidification) by treated *S. aureus* was inhibited, including lactose and maltose. The treated cells were not able to acidify N-acetylglucosamine. The results also showed that the enzyme arginine dihydrolase was inhibited.

Table 1. API Staph biochemical profile of untreated *S. aureus* and *S. aureus* treated with AQT at concentrations of 5.2 and 10.4 µg/mL.

Test	Active ingredients	Reactions/enzymes	Result		*S. aureus*		
			Negative	Positive	Control	5.2 µg/mL	10.4 µg/mL
0	No substrate	Negative control	Red	-	-	-	-
GLU	D-glucose	(Positive control) (D-GLUcose)	Red	Yellow	+	+	+
FRU	D-fructo	Acidification(D-FRUctose)			+	+	+
MNE	D-mannose	acidification (D-ManNosE)			+	+	+
MAL	D-malto	acidification (MALtose)			+	-	-
LAC	D-lactose (bovine origin)	acidification (LACtose)			+	-	-
TRE	D-trehalose	acidification (D-TREhalose)			+	+	+
MAN	D-mannitol	acidification (D-MANnitol)			+	+	+
XLT	xylitol	acidification (XyLiTol)			-	-	-
MEL	D-melibiose	acidification (D-MELibiose)			-	-	-
NIT	potassium nitrate	Reduction of NITrates to nitrites	Colorless	Light pink red	+	+	+
PAL	ß-naphthyl phosphate	ALkaline Phosphatase	Yellow	Violet	NT	NT	NT
VP	sodium pyruvate	Acetyl-methyl-carbinol production (Voges Proskauer)	Colorless-light pink	Violet-pink	+	+	+
RAF	D-raffinose	acidification (RAFfinose)	Red	Yellow	-	-	-
XYL	D-xylose	acidification (XYLose)			-	-	-
SAC	D-saccharose (sucrose)	acidification (SACcharose)			+	-	-
MDG	methyl-αD glucopyranoside	acidification (Methyl-αD Glucopyranoside)			-	-	-
NAG	N-acetyl-glucosamine	acidification (N-Acetyl-Glucosamine)			+	-	-
ADH	L-arginine	Arginine DiHydrolase	Yellow	Orange-red	+	-	-
URE	urea	UREase	Yellow	Red-violet	+	+	+

Lipase Activity

The percentage of colonies (CFU) presenting active lipase for untreated *S. aureus* and *S. aureus* treated with AQT at concentrations of 5.2 and 10.4 µg/mL are shown in Table 2. The results showed that the lipase activity of *S. aureus* treated with AQT was not affected. The percentage of *S. aureus* colonies presenting active lipase in the untreated culture was 88.2%, while the percentages for cultures treated with 5.2 and 10.4 µg/mL RnD1c were 86.7% and 87.1%, respectively.

Table 2. Percentage of *S. aureus* colonies (CFU) presenting active lipase activity in untreated and AQT-treated cultures.

S. aureus	Lipase activity (%)*
Control	88.2±1.99
RnD1c 5.2 µg/mL	86.7±4.41
RnD1c 10.4 µg/mL	87.1±3.85

*Lipase activity= (CFU representing lipase activity/ total CFU)×100%
Data represent the mean of triplicate readings and expressed as Mean±SD.

Leakage of ATP

To investigate the effect of AQT on the intracellular ATP of *S. aureus*, the intracellular and extracellular ATP concentrations at three different incubation times were measured qualitatively. As shown in Figure 12, AQT causes massive leakage of ATP from the cell. At two different concentrations (5.2 and 10.4 µg/mL), the intracellular ATP level of treated *S. aureus* was decreased, while the extracellular ATP level increased significantly compared to untreated *S. aureus*.

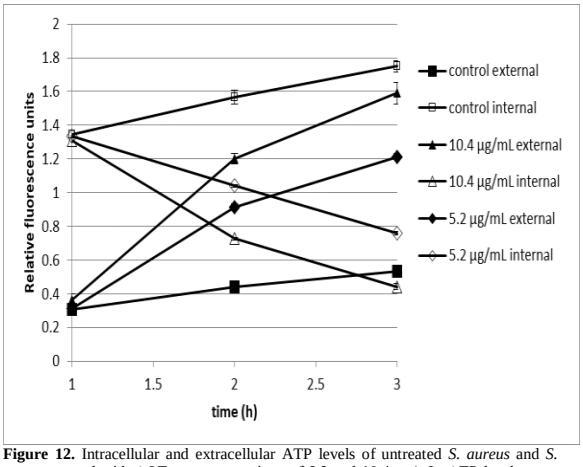

Figure 12. Intracellular and extracellular ATP levels of untreated *S. aureus* and *S. aureus* treated with AQT at concentrations of 5.2 and 10.4 µg/mL. ATP levels were measured at different incubation times to assess membrane integrity and cellular energy leakage.

Membrane Depolarization

The fluorescent probe $DiSC_3(5)$ was used to measure the membrane potential of *S. aureus*. $DiSC_3(5)$ is a self-quenching fluorescent dye once it enters the cell. If an antibiotic forms channels or damages the cell membrane, the membrane potential will be dissipated, and the dye will leak into the medium, causing an increase in fluorescence absorption. As shown in Figure 13, the treatment of *S. aureus* with AQT at two different concentrations (5.2 and 10.4 µg/mL) caused depolarization of the cell membrane. The *S. aureus* treated with 10.4 µg/mL of AQT showed significant membrane depolarization compared to the depolarization observed with 5.2 µg/mL. Tetracycline, which was used as a negative control, exhibited no depolarization effect.

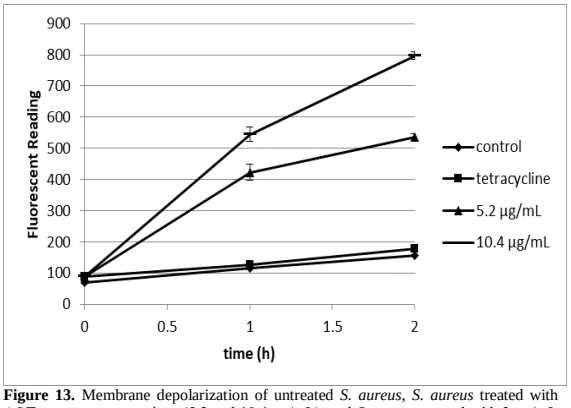

Figure 13. Membrane depolarization of untreated *S. aureus*, *S. aureus* treated with AQT at two concentrations (5.2 and 10.4 µg/mL), and *S. aureus* treated with 3 µg/mL tetracycline. Membrane potential changes were measured using the $DiSC_3(5)$ fluorescent dye. An increase in fluorescence indicates loss of membrane potential due to membrane disruption.

DISCUSSION

AQT was bacteriostatic at a concentration of 2.6 µg/mL and bactericidal at the concentration of 5.2 µg/mL. Time-kill analysis was performed for *S. aureus* treated with AQT at concentrations equal to MIC value (2.6 µg/mL), ½ MIC value (1.3 µg/mL), 2× MIC value (5.2 µg/mL), and 4× MIC value (10.4 µg/mL). The results showed that AQT decreases the surviving cell numbers dramatically. *S. aureus* was killed within 6 to 8 hours when it was treated with AQT at concentrations equal to 5.2 and 10.4 µg/mL, respectively. Prolonged exposure to AQT results in the loss of viability when *S. aureus* was treated at lower concentrations. Therefore, concentrations of AQT that are able to decrease the surviving cell numbers and cause killing (5.2 and 10.4 µg/mL) were used in most of the following experiments to investigate the effect of AQT on viable affected cells.

The scanning electron microscopy (SEM) is usually applied to evaluate the effect of certain antibiotics on the bacterial cell envelope (Parthasarathi et al., 2025). The signs of effects are usually described according to the size, shape, and texture of the treated cells compared to untreated cells. Equally important is to

describe the degree of damage of the tested cells. The latter may include partial damage or complete damage of the cells. Cell deformation, loss of membrane integrity, and the presence of odd or unusual cell structures, such as the presence of projections and bud scars, are all signs of partial damage. While partial damage of the cell refers to the damage of the cell envelope including the cell wall and the cell membrane, complete damage reveals lysis of the cell. The presence of cell contents in such forms as cell debris or aggregations are the signs of complete damage (Aiemsaard et al., 2011; Cushnie et al., 2016; Ismail et al., 2024). In this study, the effect of AQT on *S. aureus* cell envelope was examined using SEM. *S. aureus* was exposed to AQT at two different concentrations. At the lower concentration (5.2 µg/mL), partial damage was observed, while at the higher concentration (10.4 µg/mL) complete damage of the cell was observed. According to the observed signs, AQT appears to cause alterations in the cell wall and cell membrane and leads to lysis of the cell.

Several reports showed that there is a correlation between the modes of action of antibiotics and the morphological alterations of bacteria. Antibiotics such as penicillin (β-lactam antibiotics), quinolones, oxolonic acid, novobiocin, nitrofurantoin, sulfonamides, and trimethoprim were reported previously to alter the Gram-negative morphology from bacillus shape to filaments or spherical shape. While in Gram-positive bacteria such as *S. aureus*, antibiotics usually lead to enlargement of the cells but not changing their morphology. In both cases, each abnormal progeny cell consists of several cells derived from a single parent cell prevented from separating by failure to lyse adjoining cross walls (Lorian, 1999; Nikola et al., 2022; van Teeseling et al., 2017). Thus, morphological abnormality of the bacterial cell is a sign of cessation of cell division, and it may suggest that the DNA and protein synthesis were inhibited (Figueroa-Cuilan et al., 2021). Ulvatne et al. (2004) reported that the inhibition of DNA and protein synthesis induces morphological abnormality (Ulvatne et al., 2004). The morphological changes observed here may imply that AQT is not targeting DNA or protein synthesis since no enlargement in the treated *S. aureus* was observed. Moreover, lipase activity of *S. aureus* was investigated to detect the effect of AQT on protein synthesis. Lipase activity of *S. aureus* treated with AQT and with antibiotic inhibiting protein synthesis was compared with untreated *S. aureus*. The finding revealed that AQT showed no significant effect on protein synthesis, whereas chloramphenicol significantly inhibited lipase activity. Inhibition of exo-protein synthesis is known only with antibiotics that block protein synthesis; those that affect the cell envelope have a stimulatory effect on the synthesis of most exo-proteins (Herbert et al., 2001; Zheng et al., 2021).

In order to confirm if AQT is targeting the cell wall or the cell membrane of *S. aureus*, an autolysis assay was performed. It is well known that cell wall-active antibiotics induce autolysis of bacteria such as *S. aureus*. Treatment of *S. aureus* with a cell wall-active antibiotic mediates cell killing and lysis (Kawai et al., 2023). In fact, lysis of bacteria results from direct solubilization of the cell membrane, membrane deenergization, or inhibition of penicillin-binding proteins. However, lysis by solubilization of the cell membrane does not result from cell wall degradation; lysis by membrane deenergization and inhibition of penicillin-binding proteins results from triggering the autolytic enzymes. Cell wall-active antibiotics trigger cell autolysins, which are hydrolase enzymes that degrade the peptidoglycan of the cell wall (Keller & Dörr, 2023). In this study, the autolysis of *S. aureus* treated with AQT is shown to be analogous to the autolysis of *S. aureus* treated with ampicillin. However, the autolysis rate of *S. aureus* treated with chloramphenicol, which is a protein synthesis inhibitor, showed very little change compared to the untreated culture. Reinicke et al. (1983) reported that chloramphenicol causes thickening of the *S. aureus* cell wall and decreases susceptibility of cells to lysozyme and a decrease in autolysis (Reinicke et al., 1983).

The physiological examination of treated *S. aureus* using the API Staph test system showed that *S. aureus* was unable to acidify NAG (N-acetylglucosamine). Imada et al. (1979) reported that the deficiency of NAG interrupts cell wall synthesis. The mutant strains of *S. aureus* and *E. coli* which lack glucosamine-6-phosphate synthetase were unable to synthesize cell wall components (Dörr, 2021; Imada et al., 1977; Stefaniak et al., 2022).

For understanding the mechanism of action of AQT, the ability of AQT to alter the permeability of *S. aureus* membrane was evaluated using the crystal violet assay and PI assay. The effect of AQT on the cell membrane permeability was evidenced by the uptake of the dye crystal violet (CV). A significant CV uptake was observed when *S. aureus* was treated with AQT compared to the control culture. This indicates that AQT altered *S. aureus* membrane permeability, making it highly permeable to solutes. Similar results were observed using the PI assay. However, chloramphenicol and streptomycin showed no effect on the uptake of CV and PI since the mode of action of both of them is targeting protein synthesis. Antibiotics targeting the cell membrane usually enhance membrane fluidity and permeability, alter membrane-embedded proteins, and disrupt ion transport processes, leading to inhibition of respiration (Kumar & Engle, 2023; Panda et al., 2022).

The results of UV-absorbing materials further support the evidence that AQT caused disintegration of the cell membrane. Leakage of 260 and 280 nm-absorbing materials suggests that the cell membrane of *S. aureus* was damaged and caused leakage of intracellular constituents like nucleic acids and proteins. The SDS-PAGE pattern for the total cell proteins also supports this idea. The release of intracellular constituents might be due to cell lysis or the formation of non-selective pores in the cell membrane (Moo et al., 2021; Segovia et al., 2021). An important consequence of membrane alteration of bacteria exposed to antibiotics is the alteration in ion transport processes. Treatment of *S. aureus* cells with AQT resulted in the leakage of potassium and calcium ions. Many studies showed that the leakage of these ions occurred immediately through the formation of non-selective pores (Bhaumik et al., 2024; Devi et al., 2010; Müller et al., 2016).

The leakage of ions like potassium and calcium may be followed by ATP hydrolysis, which may cause membrane depolarization. The effect of AQT on the ATP status of *S. aureus* showed that the intracellular ATP of the treated *S. aureus* was decreased while the extracellular ATP was increased. Due to ATP hydrolysis or ATP efflux that occurred by the action of AQT, the cells would attempt to re-accumulate the lost ions by ATP-dependent uptake systems. This will cause membrane depolarization (Bhaumik et al., 2024; Stautz et al., 2021; Zhou et al., 2008). In the bacterial cells, the cell hydrolyzes more ATP to maintain the balance of the ion gradient and then utilizes the ion gradient to produce energy. Certain antibiotics interrupt this balance, thus leading to loss of membrane potential and to cell death (te Winkel et al., 2016; Vestergaard et al., 2022). However, the investigation of the physiological status of treated *S. aureus* showed that arginine dihydrolase, the enzyme involved in ATP generation, was inhibited by the action of AQT. The inhibition of this enzyme could inhibit dephosphorylation of carbamoyl phosphate and then inhibit ATP production (Pols et al., 2021; Reslane et al., 2024). When carbohydrate nutrient is at low concentration, the cells might overcome this starvation status by using carbamoyl phosphate, which is a substrate of arginine dihydrolase, to generate ATP. ATP generation by arginine dihydrolase occurs in three steps: degradation of arginine, by the action of arginine dihydrolase, to produce citrulline and ammonia; cleavage of citrulline, by the action of ornithine transcarbamoylase, to produce carbamoyl phosphate and ornithine; then, dephosphorylation of carbamoyl phosphate, by the action of carbamate kinase, will lead to the production of ATP, ammonia, and carbon dioxide (Novák et al., 2016; Pols et al., 2021).

In this study, $DiSC_3(5)$ assay was used to investigate the membrane depolarization (potential) of *S. aureus*. The fluorescent probe $DiSC_3(5)$ is distributed between cells and medium depending on the cytoplasmic membrane potential. Once $DiSC_3(5)$ penetrates inside the cells, it self-quenches its own fluorescence. If the antibiotic forms channels or otherwise disrupts the membrane, the membrane potential will be dissipated, and $DiSC_3(5)$ will be released into the medium, causing the fluorescence to increase (Gray et al., 2024; te Winkel et al., 2016). The results showed an increase in the fluorescent absorbance, indicating that AQT caused depolarization of the cell membrane.

Conclusion:
This study investigated several cellular factors to elucidate the mode of action of AQT. It is clear that AQT leads to the efflux of several intracellular components and membrane potential dissipation, followed by inhibition of all energy-dependent cellular processes. AQT also leads to the triggering of autolytic enzymes and the inhibition of NAG synthesis. The results may imply that AQT exhibits multiple antibacterial mechanisms, including acting upon the cell membrane and cell wall.

Funding
The study was not funded by external sources aside the author.

Data Availability
All data generated are represented in this manuscript.

Conflict of Interest
The authors declare no conflict of interest in this study

Author Contribution
SI conceived and designed the study. SI, SS, and DS performed the experiments and data analysis. SS drafted the initial manuscript. All authors reviewed and approved the final version of the manuscript.

Declaration of Generative AI and AI-Assisted Technologies in the Writing Process
The authors declare that no AI-assisted technologies or AI-generated data were used in this study.

References

Aiemsaard, J., Aiumlamai, S., Aromdee, C., Taweechaisupapong, S., and Khunkitti, W. (2011). The effect of lemongrass oil and its major components on clinical isolate mastitis pathogens and their mechanisms of action on Staphylococcus aureus DMST 4745. *Research in Veterinary Science*, **91**(3), e31–e37. https://doi.org/https://doi.org/10.1016/j.rvsc.2011.01.012

Allison, D. G., and Lambert, P. A. (2024). *Chapter 31 - Modes of action of antibacterial agents* (Y.-W. Tang, M. Y. Hindiyeh, D. Liu, A. Sails, P. Spearman, & J.-R. B. T.-M. M. M. (Third E. Zhang (eds.); pp. 597–614). Academic Press. https://doi.org/https://doi.org/10.1016/B978-0-12-818619-0.00133-7

Ann-Britt, S., Margareth, S., Ireny, A. N., Gabriela, M. R., Aysha, A., and Michaela, W. (2024). Dissecting antibiotic effects on the cell envelope using bacterial cytological profiling: a phenotypic analysis starter kit. *Microbiology Spectrum*, **12**(3), e03275-23. https://doi.org/10.1128/spectrum.03275-23

Barros, J., Conceição, M., Neto, N., Costa, A., Siqueira, J., Basílio, I., and Souza, E. (2009). Interference of Origanum vulgare L. essential oil on the growth and some physiological characteristics of Staphylococcus aureus strains isolated from foods. *LWT - Food Science and Technology*, **42**(6), 1139–1143. https://doi.org/10.1016/j.lwt.2009.01.010

Benli, M., Yiğit, N., Geven, F., Güney, K., and Bingöl, Ü. (2008). Antimicrobial activity of endemic Crataegus tanacetifolia (Lam.) Pers and observation of the inhibition effect on bacterial cells. *Cell Biochemistry and Function*, **26**(8), 844–851. https://doi.org/https://doi.org/10.1002/cbf.1515

Bhaumik, K. N., Spohn, R., Dunai, A., Daruka, L., Olajos, G., Zákány, F., Hetényi, A., Pál, C., and Martinek, T. A. (2024). Chemically diverse antimicrobial peptides induce hyperpolarization of the E. coli membrane. *Communications Biology*, **7**(1), 1264. https://doi.org/10.1038/s42003-024-06946-4

Brötz-Oesterhelt, H., and Brunner, N. A. (2008). How many modes of action should an antibiotic have? *Current Opinion in Pharmacology*, **8**(5), 564–573. https://doi.org/10.1016/j.coph.2008.06.008

Carson, C. ., Mee, B. ., and Riley, T. . (2002). Mechanism of Action of Melaleuca alternifolia (Tea Tree) Oil on Staphylococcus aureus Determined by Time-Kill, Lysis, Leakage, and Salt Tolerance Assays and Electron Microscopy. *Antimicrobial Agents and Chemotherapy*, **46**(6), 1914–1920. https://doi.org/10.1128/aac.46.6.1914-1920.2002

Chen, S., Qin, S., Li, R., Qu, Y., Ampomah-Wireko, M., Nininahazwe, L., Wang, M., Gao, C., and Zhang, E. (2024). Design, synthesis and antibacterial evaluation of low toxicity amphiphilic-cephalosporin derivatives. *European Journal of Medicinal Chemistry*, **268**, 116293. https://doi.org/https://doi.org/10.1016/j.ejmech.2024.116293

Cushnie, T. P. T., O'Driscoll, N. H., and Lamb, A. J. (2016). Morphological and ultrastructural changes in bacterial cells as an indicator of antibacterial mechanism of action. *Cellular and Molecular Life Sciences*, **73**(23), 4471–4492. https://doi.org/10.1007/s00018-016-2302-2

Dalhoff, A. (2021). Selective toxicity of antibacterial agents—still a valid concept or do we miss chances and ignore risks? *Infection*, **49**(1), 29–56. https://doi.org/10.1007/s15010-020-01536-y

de León, L., López, M. R., and Moujir, L. (2010). Antibacterial properties of zeylasterone, a triterpenoid isolated from Maytenus blepharodes, against Staphylococcus aureus. *Microbiological Research*, **165**(8), 617–626. https://doi.org/https://doi.org/10.1016/j.micres.2009.12.004

Devi, K. P., Nisha, S. A., Sakthivel, R., and Pandian, S. K. (2010). Eugenol (an essential oil of clove) acts as an antibacterial agent against Salmonella typhi by disrupting the cellular membrane. *Journal of Ethnopharmacology*, **130**(1), 107–115. https://doi.org/https://doi.org/10.1016/j.jep.2010.04.025

Dörr, T. (2021). Understanding tolerance to cell wall–active antibiotics. *Annals of the New York Academy of Sciences*, **1496**(1), 35–58. https://doi.org/https://doi.org/10.1111/nyas.14541

Figueroa-Cuilan, W. M., Randich, A. M., Dunn, C. M., Santiago-Collazo, G., Yowell, A., and Brown, P. J. B. (2021). Diversification of LytM Protein Functions in Polar Elongation and Cell Division of Agrobacterium tumefaciens. *Frontiers in Microbiology*, **12**. https://www.frontiersin.org/journals/microbiology/articles/10.3389/fmicb.2021.729307

Fleury, B., Kelley, W. L., Lew, D., Götz, F., Proctor, R. A., and Vaudaux, P. (2009). Transcriptomic and metabolic responses of Staphylococcus aureus exposed to supra-physiological temperatures. *BMC Microbiology*, **9**(1), 76. https://doi.org/10.1186/1471-2180-9-76

Friedrich, C. L., Moyles, D., Beveridge, T. J., and Hancock, R. E. (2000). Antibacterial action of structurally diverse cationic peptides on gram-positive bacteria. *Antimicrobial Agents and Chemotherapy*, **44**(8), 2086–2092. https://doi.org/10.1128/AAC.44.8.2086-2092.2000

Gauri, S. S., Mandal, S. M., Pati, B. R., and Dey, S. (2011). Purification and structural characterization of a novel antibacterial peptide from Bellamya bengalensis: activity against ampicillin and chloramphenicol resistant Staphylococcus epidermidis. *Peptides*, **32**(4), 691–696. https://doi.org/10.1016/j.peptides.2011.01.014

Gray, D. A., Wang, B., Sidarta, M., Cornejo, F. A., Wijnheijmer, J., Rani, R., Gamba, P., Turgay, K., Wenzel, M., Strahl, H., and Hamoen, L. W. (2024). Membrane depolarization kills dormant Bacillus subtilis cells by generating a lethal dose of ROS. *Nature Communications*, **15**(1), 6877. https://doi.org/10.1038/s41467-024-51347-0

Hanaki, H., Kuwahara-Arai, K., Boyle-Vavra, S., Daum, R. S., Labischinski, H., and Hiramatsu, K. (1998). Activated cell-wall synthesis is associated with vancomycin resistance in methicillin-resistant Staphylococcus aureus clinical strains Mu3 and Mu50. *The Journal of Antimicrobial Chemotherapy*, **42**(2), 199–209. https://doi.org/10.1093/jac/42.2.199

Herbert, S., Barry, P., and Novick, R. P. (2001). Subinhibitory clindamycin differentially inhibits transcription of exoprotein genes in Staphylococcus aureus. *Infection and Immunity*, **69**(5), 2996–3003. https://doi.org/10.1128/IAI.69.5.2996-3003.2001

Ideker, T., Galitski, T., and Hood, L. (2001). A new approach to decoding life: systems biology. *Annual Review of Genomics and Human Genetics*, **2**(1), 343–372. https://doi.org/10.1146/annurev.genom.2.1.343

Idid, S., Saad, S., and Susanti, D. (2024). Bioassay-Guided Isolation of Antimicrobial Compounds from Marine Sponge Neopetrosia exigua. *Journal of Basic and Applied Research in Biomedicine*, **10**(1 SE-Original Article), 50–58. https://doi.org/10.51152/jbarbiomed.v10i1.235

Imada, A., Nozaki, Y., Kawashima, F., and Yoneda, M. (1977). Regulation of glucosamine utilization in Staphylococcus aureus and Escherichia coli. *Journal of General Microbiology*, **100**(2), 329–337. https://doi.org/10.1099/00221287-100-2-329

Ismail, B. B., Wang, W., Ayub, K. A., Guo, M., and Liu, D. (2024). Advances in microscopy-based techniques applied to the antimicrobial resistance of foodborne pathogens. *Trends in Food*

Science & Technology, **152**, 104674. https://doi.org/https://doi.org/10.1016/j.tifs.2024.104674

Joshi, S., Bisht, G. S., Rawat, D. S., Kumar, A., Kumar, R., Maiti, S., and Pasha, S. (2010). Interaction studies of novel cell selective antimicrobial peptides with model membranes and E. coli ATCC 11775. *Biochimica et Biophysica Acta*, **1798**(10), 1864–1875. https://doi.org/10.1016/j.bbamem.2010.06.016

Kawai, Y., Kawai, M., Mackenzie, E. S., Dashti, Y., Kepplinger, B., Waldron, K. J., and Errington, J. (2023). On the mechanisms of lysis triggered by perturbations of bacterial cell wall biosynthesis. *Nature Communications*, **14**(1), 4123. https://doi.org/10.1038/s41467-023-39723-8

Keller, M. R., and Dörr, T. (2023). Chapter Four - Bacterial metabolism and susceptibility to cell wall-active antibiotics. In R. K. Poole & D. J. B. T.-A. in M. P. Kelly (Eds.), *Advances in Microbial Physiology* (Vol. 83, pp. 181–219). Academic Press. https://doi.org/https://doi.org/10.1016/bs.ampbs.2023.04.002

Kumar, G., and Engle, K. (2023). Natural products acting against S. aureus through membrane and cell wall disruption. *Natural Product Reports*, **40**(10), 1608–1646. https://doi.org/10.1039/D2NP00084A

Lorian, V. (1999). Modes of Action of Antibiotics and Bacterial Structure: Bacterial Mass Versus their Numbers. In *Handbook of Animal Models of Infection* (pp. 105–116). Elsevier.

Mani, N., Tobin, P., and Jayaswal, R. K. (1993). Isolation and characterization of autolysis-defective mutants of Staphylococcus aureus created by Tn917-lacZ mutagenesis. *Journal of Bacteriology*, **175**(5), 1493–1499. https://doi.org/10.1128/jb.175.5.1493-1499.1993

Moo, C.-L., Osman, M. A., Yang, S.-K., Yap, W.-S., Ismail, S., Lim, S.-H.-E., Chong, C.-M., and Lai, K.-S. (2021). Antimicrobial activity and mode of action of 1,8-cineol against carbapenemase-producing Klebsiella pneumoniae. *Scientific Reports*, **11**(1), 20824. https://doi.org/10.1038/s41598-021-00249-y

Müller, A., Wenzel, M., Strahl, H., Grein, F., Saaki, T. N. V, Kohl, B., Siersma, T., Bandow, J. E., Sahl, H.-G., Schneider, T., and Hamoen, L. W. (2016). Daptomycin inhibits cell envelope synthesis by interfering with fluid membrane microdomains. *Proceedings of the National Academy of Sciences*, **113**(45), E7077–E7086. https://doi.org/10.1073/pnas.1611173113

Nikola, O., Diana, S., and Shiladitya, B. (2022). Antibiotic Resistance via Bacterial Cell Shape-Shifting. *MBio*, **13**(3), e00659-22. https://doi.org/10.1128/mbio.00659-22

Nostro, A., Bisignano, G., Angela Cannatelli, M., Crisafi, G., Paola Germanò, M., and Alonzo, V. (2001). Effects of Helichrysum italicum extract on growth and enzymatic activity of Staphylococcus aureus. *International Journal of Antimicrobial Agents*, **17**(6), 517–520. https://doi.org/10.1016/s0924-8579(01)00336-3

Novák, L., Zubáčová, Z., Karnkowska, A., Kolisko, M., Hroudová, M., Stairs, C. W., Simpson, A. G. B., Keeling, P. J., Roger, A. J., Čepička, I., and Hampl, V. (2016). Arginine deiminase pathway enzymes: evolutionary history in metamonads and other eukaryotes. *BMC Evolutionary Biology*, **16**(1), 197. https://doi.org/10.1186/s12862-016-0771-4

Panda, G., Dash, S., and Sahu, S. K. (2022). Harnessing the Role of Bacterial Plasma Membrane Modifications for the Development of Sustainable Membranotropic Phytotherapeutics. In *Membranes* (Vol. 12, Issue 10). https://doi.org/10.3390/membranes12100914

Parthasarathi, S., Chaudhury, A., Swain, A., and Basu, J. K. (2025). Microscopy Insights as an Invaluable Tool for Studying Antimicrobial Interactions with Bacterial Membranes. *ChemistrySelect*, **10**(21), e02345. https://doi.org/https://doi.org/10.1002/slct.202502345

Pols, T., Singh, S., Deelman-Driessen, C., Gaastra, B. F., and Poolman, B. (2021). Enzymology of the pathway for ATP production by arginine breakdown. *The FEBS Journal*, **288**(1), 293–309. https://doi.org/10.1111/febs.15337

Priyamvada, P., Debroy, R., Anbarasu, A., and Ramaiah, S. (2022). A comprehensive review on genomics, systems biology and structural biology approaches for combating antimicrobial resistance in ESKAPE pathogens: computational tools and recent advancements. *World Journal of Microbiology and Biotechnology*, **38**(9), 153. https://doi.org/10.1007/s11274-022-03343-z

Reinicke, B., Blümel, P., and Giesbrecht, P. (1983). Reduced degradability by lysozyme of staphylococcal cell walls after chloramphenicol treatment. *Archives of Microbiology*, **135**(2), 120–124. https://doi.org/10.1007/BF00408020

Ren, F., Li, Y., Chen, W., Chen, W., Chen, H., and Zhang, M. (2024). Antimicrobial mechanism of linalool against Vibrio parahaemolyticus and its application in black tiger shrimp (Penaeus monodon). *Food Bioscience*, **60**, 104283. https://doi.org/https://doi.org/10.1016/j.fbio.2024.104283

Reslane, I., Watson, G. F., Handke, L. D., and Fey, P. D. (2024). Regulatory dynamics of arginine metabolism in Staphylococcus aureus. *Biochemical Society Transactions*, **52**(6), 2513–2523. https://doi.org/10.1042/BST20240710

Segovia, R., Solé, J., Marqués, A. M., Cajal, Y., and Rabanal, F. (2021). Unveiling the Membrane and Cell Wall Action of Antimicrobial Cyclic Lipopeptides: Modulation of the Spectrum of Activity. In *Pharmaceutics* (Vol. 13, Issue 12). https://doi.org/10.3390/pharmaceutics13122180

Sharma, V., Das, R., Mehta, D. K., Sharma, D., Aman, S., and Khan, M. U. (2025). Quinolone scaffolds as potential drug candidates against infectious microbes: a review. *Molecular Diversity*, **29**(1), 711–737. https://doi.org/10.1007/s11030-024-10862-4

Singh, S. B., and Barrett, J. F. (2006). Empirical antibacterial drug discovery—foundation in natural products. *Biochemical Pharmacology*, **71**(7), 1006–1015. https://doi.org/https://doi.org/10.1016/j.bcp.2005.12.016

Sladić, D., and Gasić, M. J. (2006). Reactivity and biological activity of the marine sesquiterpene hydroquinone avarol and related compounds from sponges of the order Dictyoceratida. *Molecules (Basel, Switzerland)*, **11**(1), 1–33. https://doi.org/10.3390/11010001

Stautz, J., Hellmich, Y., Fuss, M. F., Silberberg, J. M., Devlin, J. R., Stockbridge, R. B., and Hänelt, I. (2021). Molecular Mechanisms for Bacterial Potassium Homeostasis. *Journal of Molecular Biology*, **433**(16), 166968. https://doi.org/https://doi.org/10.1016/j.jmb.2021.166968

Stefaniak, J., Michał G., N., Marek, W., Sławomir, M., and and Skwarecki, A. S. (2022). Inhibitors of glucosamine-6-phosphate synthase as potential antimicrobials or antidiabetics – synthesis and properties. *Journal of Enzyme Inhibition and Medicinal Chemistry*, **37**(1), 1928–1956. https://doi.org/10.1080/14756366.2022.2096018

te Winkel, J. D., Gray, D. A., Seistrup, K. H., Hamoen, L. W., and Strahl, H. (2016). Analysis of Antimicrobial-Triggered Membrane Depolarization Using Voltage Sensitive Dyes. *Frontiers in Cell and Developmental Biology*, **4**. https://www.frontiersin.org/journals/cell-and-developmental-biology/articles/10.3389/fcell.2016.00029

Togashi, N., Shiraishi, A., Nishizaka, M., Matsuoka, K., Endo, K., Hamashima, H., and Inoue, Y. (2007). Antibacterial activity of long-chain fatty alcohols against Staphylococcus aureus. *Molecules (Basel, Switzerland)*, **12**(2), 139–148. https://doi.org/10.3390/12020139

Ul Haq, I., Rafael, P. V., William Gustavo, L., Maria Elena, de L., and and Krukiewicz, K. (2024). Antimicrobial polymers: elucidating the role of functional groups on antimicrobial activity. *Arab Journal of Basic and Applied Sciences*, **31**(1), 325–344. https://doi.org/10.1080/25765299.2024.2366543

Ulvatne, H., Samuelsen, Ø., Haukland, H. H., Krämer, M., and Vorland, L. H. (2004). Lactoferricin B inhibits bacterial macromolecular synthesis in Escherichia coli and Bacillus subtilis. *FEMS Microbiology Letters*, **237**(2), 377–384. https://doi.org/10.1016/j.femsle.2004.07.001

van Teeseling, M. C. F., de Pedro, M. A., and Cava, F. (2017). Determinants of Bacterial Morphology: From Fundamentals to Possibilities for Antimicrobial Targeting. *Frontiers in Microbiology*, **8**. https://www.frontiersin.org/journals/microbiology/articles/10.3389/fmicb.2017.01264

Vestergaard, M., Bald, D., and Ingmer, H. (2022). Targeting the ATP synthase in bacterial and fungal pathogens: beyond Mycobacterium tuberculosis. *Journal of Global Antimicrobial Resistance*, **29**, 29–41. https://doi.org/https://doi.org/10.1016/j.jgar.2022.01.026

Zhao, W., Chengwei, Y., Ning, Z., Yuanyuan, P., Ying, M., Keru, G., Xia, L., Xiaohui, L., Xijian, L., Yumin, L., Songkai, L., and and Zhao, L. (2023). Menthone Exerts its Antimicrobial Activity Against Methicillin Resistant Staphylococcus aureus by Affecting Cell Membrane Properties and Lipid Profile. *Drug Design, Development and Therapy*, **17**(null), 219–236. https://doi.org/10.2147/DDDT.S384716

Zheng, X., Marsman, G., Lacey, K. A., Chapman, J. R., Goosmann, C., Ueberheide, B. M., and Torres, V. J. (2021). The cell envelope of Staphylococcus aureus selectively controls the sorting of virulence factors. *Nature Communications*, **12**(1), 6193. https://doi.org/10.1038/s41467-021-26517-z

Zhou, K., Zhou, W., Li, P., Liu, G., Zhang, J., and Dai, Y. (2008). Mode of action of pentocin 31-1: An antilisteria bacteriocin produced by Lactobacillus pentosus from Chinese traditional ham. *Food Control*, **19**(8), 817–822. https://doi.org/https://doi.org/10.1016/j.foodcont.2007.08.008